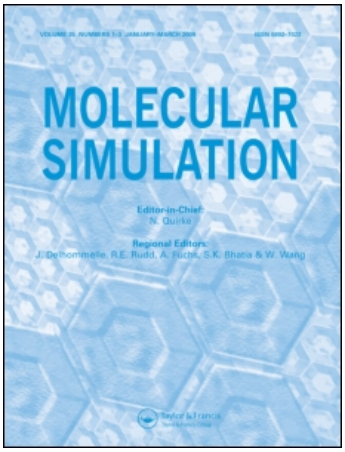

Molecular Simulation
Publication details, including instructions for authors and subscription information:
http://www.informaworld.com/smpp/title~content=t713644482

Molecular simulation study of the glass transition for a flexible model of linear alkanes

Mariana Martín-Betancourt[a]; José M. Romero-Enrique[a]; Luis F. Rull[a]
[a] Departamento de Física Atómica, Molecular y Nuclear, Area de Física Teórica, Universidad de Sevilla, Sevilla, Spain

To cite this Article Martín-Betancourt, Mariana , Romero-Enrique, José M. and Rull, Luis F.(2009) 'Molecular simulation study of the glass transition for a flexible model of linear alkanes', Molecular Simulation, 35: 12, 1043 — 1050
To link to this Article: DOI: 10.1080/08927020902902767
URL: http://dx.doi.org/10.1080/08927020902902767

Molecular Simulation
Vol. 35, Nos. 12–13, October–November 2009, 1043–1050

Taylor & Francis
Taylor & Francis Group

Molecular simulation study of the glass transition for a flexible model of linear alkanes

Mariana Martín-Betancourt, José M. Romero-Enrique* and Luis F. Rull

Departamento de Física Atómica, Molecular y Nuclear, Area de Física Teórica, Universidad de Sevilla, Apartado de Correos 1065, 41080 Sevilla, Spain

(*Received 13 January 2009; final version received 9 March 2009*)

We present a molecular dynamics study in the isothermal–isobaric ensemble of a flexible model of linear *n*-alkanes for $2 \leq n \leq 10$ close to the glass transition. Our model is a modification of a realistic force field in which we have turned off the bond bending and the torsional intramolecular potentials to get the chain flexible. The glass transition is characterised by the change of slope of specific volume, as well as the vanishing of the self-diffusion coefficient and the divergence of the shear viscosity. Additionally we characterise the chain rearrangement dynamics above and close to the glass transition. Our results are in qualitative agreement with those previously obtained with more realistic models, so we conclude that the flexibility of the alkane chain does not play a dominant role in the glass transition.

Keywords: molecular dynamics; glass transition; linear *n*-alkane

1. Introduction

When a liquid is quenched below the melting temperature, it may not undergo the first-order crystallisation transition, but may remain in a metastable fluid phase: the supercooled fluid [1]. This state is the continuation of the thermodynamically stable liquid phase above the melting point, and its physical properties are similar to those of the true equilibrium liquid. If we continue cooling the system (or if we wait for a long enough time), the fluid may crystallise to the true equilibrium solid state. Alternatively, the fluid may arrest in a disordered state where the structural relaxation time becomes longer than the experimental timescale. This situation does not correspond to a truly thermodynamic transition but a dynamical one, and it is known as the glass transition. The occurrence of the glass transition depends on the cooling rate, the presence of impurities, the liquid viscosity at the melting point and the similarity of the molecular packing in the liquid and the crystal, among others [1].

In this paper, we will study the glass transition of a model for linear *n*-alkanes. This study will be carried out by molecular simulation, which has become a powerful tool to understand different phenomena experienced by the liquid matter. The glass transition on this system has been extensively studied in the literature [2–6], from the short alkanes to polyethylene. Different force fields have been proposed to model real alkanes, such as the TraPPE [7] or NERD [8]. These models include, in addition to the dispersive forces, intramolecular potentials which mimic the backbone bond, the bond bending and the torsional energies. However, the use of these force fields makes it difficult to understand the role played by each degree of freedom in the glass transition. On the other hand, more idealised models such as lattice models [9] or tangent-sphere chains [10] are useful to understand the physical grounds of phenomena such as vitrification or melting, but it is difficult to compare these with experimental data. In this paper, we present a model which reproduces the backbone structure of realistic alkane models, but we turn off the bond bending and the torsional potential to make the chain fully flexible. In this way, we expect to assess the effect of the chain flexibility on the glass transition. The paper is organised as follows. In Section 2 we present the model and the simulation techniques used in this work. In Section 3 we describe preliminary results of the glass transition and the microscopic dynamics close to the glass transition. Finally, we end up with the conclusions.

2. The model and simulation details

We have studied a flexible model of linear *n*-alkanes based on the NERD force field [8]. As in the NERD model, we use a unit atom description, so the alkanes are modelled as a sequence of methylene CH_2 monomers with two methyl CH_3 monomers at the extremes, linked by rigid bonds. The bond distance between two nearest-neighbour monomers in a chain (regardless their nature) takes a fixed value $d = 1.54$ Å. In order to introduce complete flexibility in the model, we have not considered bond bending or torsional potentials. Instead, we introduce a repulsive soft potential u^{sr} between two monomers in the same chain separated by two bonds as:

$$u^{sr}(r_{ij}) = \frac{A}{r_{ij}^{12}}. \tag{1}$$

*Corresponding author. Email: enrome@us.es

ISSN 0892-7022 print/ISSN 1029-0435 online

DOI: 10.1080/08927020902902767
http://www.informaworld.com

The constant A was chosen to prevent these monomers approaching closer than the bond length d for all the temperatures considered. In particular, we choose $A = 607.1676\,\mathrm{kJ\,\AA^{12}/mol}$, so $u^{sr}(d) \sim k_\mathrm{B}T$ for $T = 410\,\mathrm{K}$. Finally, the interaction between monomers in different alkane molecules or in the same molecule but separated by three or more bonds is modelled by a Lennard-Jones potential:

$$u_{ij}(r_{ij}) = 4\varepsilon_{ij}\left[\left(\frac{\sigma_{ij}}{r_{ij}}\right)^{12} - \left(\frac{\sigma_{ij}}{r_{ij}}\right)^{6}\right]. \tag{2}$$

The potential depth ε_{ij} and the parameter σ_{ij} depend on the nature of the interacting monomers, and also on the length of the alkane chain. We have chosen the values proposed by Nath et al. [8] for the NERD model, and they are shown in Table 1. The necessity of the term given by Equation (1) is clear as we see that the Lennard-Jones diameter is larger than twice the bond length, so two monomers separated by two bonds will always overlap if there is a Lennard-Jones interaction between them.

We have run molecular dynamics (MD) computer simulations [11,12] in the isothermal–isobaric ensemble where the number of molecules N, the hydrostatic pressure p and the temperature T are fixed. We have taken $N = 500$ for all the considered cases. The simulation box is orthorhombic and periodic boundary conditions are considered in the three spatial directions. To perform these simulations, we used the Melchionna–Ciccotti–Holian algorithm [13]:

$$\begin{aligned}
&\frac{\mathrm{d}\mathbf{r}_i}{\mathrm{d}t} = \mathbf{v}_i + \eta(\mathbf{r}_i - \mathbf{R}_0); \quad \frac{\mathrm{d}\mathbf{v}_i}{\mathrm{d}t} = \frac{\mathbf{F}_i}{m_i} - (\chi + \eta)\mathbf{v}_i;\\
&\frac{\mathrm{d}V}{\mathrm{d}t} = 3\eta V; \quad \frac{\mathrm{d}\chi}{\mathrm{d}t} = \frac{N_f k_\mathrm{B}}{Q}(\mathcal{T}(t) - T) + \frac{1}{Q}(W\eta^2 - k_\mathrm{B}T);\\
&\frac{\mathrm{d}\eta}{\mathrm{d}t} = \frac{3}{W}V(\mathcal{P}(t) - p) - \chi\eta,
\end{aligned} \tag{3}$$

where $\mathbf{r}_i$ and $\mathbf{v}_i$ are the positions and velocities of the monomers, $\mathbf{R}_0$ is the position of the system centre of mass, $\mathbf{F}_i$ is the total force acting on the monomer i, and V is the volume of the system. $\mathcal{T}$ and $\mathcal{P}$ are the instantaneous temperature and pressure obtained from the kinetic energy and the virial, and T and p their applied values. Finally, η and χ are the variables associated with the thermostat and barostat, with effective masses Q and W, respectively. These masses must scale with the number of degrees of freedom N_f, so we can write $Q = N_f k_\mathrm{B} T \tau_T^2$ and $W = N_f k_\mathrm{B} T \tau_p^2$, where τ_T and τ_p are time scales related to the fluctuation correlation times for the (instantaneous) temperature and pressure, respectively. In our simulations, we considered $\tau_T = 1\,\mathrm{ps}$ and $\tau_p = 15\,\mathrm{ps}$. On the other hand, the motion equations (3) are numerically integrated with an algorithm based in the Verlet leapfrog scheme [11] by using the CCP5 DL POLY package [14] (version 2.15) with a time step of $\delta t = 0.002\,\mathrm{ps}$. In order to keep the bond lengths constant along the simulation, a modified version of the SHAKE algorithm [15] (the RDSHAKE algorithm) is used.

Our simulations are carried out in two phases. In the first phase we perform simulations at a constant pressure and temperature which is stepwise reduced by $\Delta T = 10\,\mathrm{K}$ each $\Delta t = 1000\,\mathrm{ps}$ until the glass transition is observed (other cooling protocols have been proposed in literature, see, for example, [16]). In this way we simulate the quench of the liquid at a constant cooling rate $\dot{q} = \Delta T/\Delta t = 10^{10}\,\mathrm{K/s}$. This rate is too high to allow comparison between simulations and calorimetric measurements. Instead, they may be compared with high-frequency experiments. In order to have a fluid as the first state, the initial temperature T_0 is taken to be around $2T_\mathrm{tr}$, where T_tr is the temperature of the gas–liquid-triple point, and the pressure is taken to be $p = 1.5p_\mathrm{c}$, where p_c is the experimental critical point. Table 2 shows the pressure values for different molecules. These initial states are chosen to ensure an equilibrium dense fluid as a starting point. In this cooling phase we monitor thermodynamic properties such as the specific volume at each temperature.

In a second phase, we run longer (up to 8 ns long) equilibrium NpT MD simulations from the final configurations for each temperature before it decreases in the cooling phase, in order to get the autocorrelation functions and transport coefficients such as the self-diffusion coefficient and the shear viscosity at each temperature. Note that they may be obtained also from the

Table 1. Lennard-Jones potential parameters in the NERD force field.

Molecule	$\sigma_{\mathrm{CH_2,CH_2}}$ (Å)	$\sigma_{\mathrm{CH_3,CH_3}}$ (Å)	$\varepsilon_{\mathrm{CH_2,CH_2}}$ (kJ/mol)	$\varepsilon_{\mathrm{CH_3,CH_3}}$ (kJ/mol)
Ethane	–	3.825	–	0.8365
Propane	3.93	3.857	0.3808	0.8531
n-alkanes ($n \geq 4$)	3.93	3.91	0.3808	0.8648

We show only the parameters for like monomers, the values corresponding to unlike monomers are obtained through the Lorentz-Berthelot mixing rules $\sigma_{ij} = (\sigma_{ii} + \sigma_{jj})/2$ and $\varepsilon_{ij} = \sqrt{\varepsilon_{ii}\varepsilon_{jj}}$.

Table 2. Values of pressure used in the computer simulations for each molecule.

Molecule	p (atm)
Ethane	72.16
Propane	62.87
Butane	59.20
Pentane	49.89
Hexane	44.91
Octane	36.96
Decane	31.13

cooling phase simulations, but the result will be meaningful only if the relevant autocorrelation times are much smaller than the constant temperature time in the cooling phase Δt. As the fluid approaches the glass transition, this condition may not be fulfilled. The autocorrelation functions are obtained from the time series of the corresponding properties collected in the simulation by a fast-Fourier transform technique. On the other hand, the transport coefficients are obtained from the Green-Kubo formalism in terms of integrals of the autocorrelation functions [17–19]. We will use a molecular rather than an atomistic (i.e. in terms of the monomers) description of the system in order to get the diffusion coefficient. On the other hand, an atomistic description is used to get the shear viscosity. Although the autocorrelation functions are different in both descriptions, they lead to the same transport coefficients [20]. The self-diffusion coefficient D is obtained from the velocity autocorrelation function as:

$$D = \frac{1}{3N}\sum_{i=1}^{N}\int_0^\infty \langle \mathbf{v}_i(t)\cdot\mathbf{v}_i(0)\rangle \,\mathrm{d}t, \tag{4}$$

where $\mathbf{v}_i$ here represents the velocity of the centre of mass for the molecule i. For the shear viscosity η, we use an expression from Daivis and Evans [21], which was shown to converge for isotropic systems better than other expressions used in the literature:

$$\eta = \frac{V}{10k_{\mathrm{B}}T}\sum_{\alpha,\beta}\int_0^\infty \langle P_{\alpha\beta}(t)P_{\alpha\beta}(0)\rangle \,\mathrm{d}t. \tag{5}$$

Here, the tensor $P_{\alpha\beta}$ is the traceless symmetric part of the stress tensor $\tau_{\alpha\beta}$:

$$P_{\alpha\beta} = \frac{\tau_{\alpha\beta}+\tau_{\beta\alpha}}{2} - \frac{\delta_{\alpha\beta}}{3}\sum_{\gamma}\tau_{\gamma\gamma}, \tag{6}$$

where the stress tensor is defined as:

$$\tau_{\alpha\beta} = \frac{1}{V}\left(\sum_{i=1}^{Nn} m_i v_i^\alpha v_i^\beta + \sum_{i<j} r_{ij}^\alpha F_{ij}^\beta\right). \tag{7}$$

As in this expression we use an atomistic description, v_i^α is the α component of the velocity of the monomer i. The vector $\mathbf{r}_{ij}$ is the relative position of the monomer i with respect to the monomer j and $\mathbf{F}_{ij}$ is the total force which the monomer j exerts on the monomer i.

Finally, we characterise the chain conformation rearrangements with the autocorrelation functions of a series of unit vectors [22]:

$$\begin{aligned}\mathbf{b}_i &= \frac{\mathbf{r}_{i+1}-\mathbf{r}_i}{|\mathbf{r}_{i+1}-\mathbf{r}_i|}, \quad \mathbf{c}_i = \frac{\mathbf{b}_{i+1}+\mathbf{b}_i}{|\mathbf{b}_{i+1}+\mathbf{b}_i|},\\ \mathbf{o}_i &= \frac{\mathbf{b}_{i+1}\times\mathbf{b}_i}{|\mathbf{b}_{i+1}\times\mathbf{b}_i|}, \quad \mathbf{s}_i = \frac{\mathbf{b}_{i+1}-\mathbf{b}_i}{|\mathbf{b}_{i+1}-\mathbf{b}_i|}.\end{aligned} \tag{8}$$

Here, $\mathbf{r}_i$ is the position vector of the monomer i of the chain, so $\mathbf{b}_i$ is the bond unit vector. The unit vectors $\mathbf{c}_i$, $\mathbf{o}_i$ and $\mathbf{s}_i$ are the chord, out-of-plane and bisector vectors, respectively, and they are useful to monitor the structural rearrangements of a chain segment formed by two consecutive bonds. For each unit vector $\mathbf{e}$ (where $\mathbf{e}$ can be any of the unit vectors defined in (8)), we define two orientational autocorrelation functions:

$$g_1^{\mathbf{e}}(t) = \langle P_1(\mathbf{e}(0)\cdot\mathbf{e}(t))\rangle = \langle \mathbf{e}(0)\cdot\mathbf{e}(t)\rangle, \tag{9}$$

$$g_2^{\mathbf{e}}(t) = \langle P_2(\mathbf{e}(0)\cdot\mathbf{e}(t))\rangle = \frac{3\langle(\mathbf{e}(0)\cdot\mathbf{e}(t))^2\rangle - 1}{2}, \tag{10}$$

where $P_k(x)$ is the kth-degree Legendre polynomial.

3. Results

In order to get a first estimate for the glass transition, we monitorised the specific volume obtained for each temperature in the cooling phase. At the glass transition, we expected to observe a sudden change in the slope of the specific volume as a function of the temperature, which corresponds to a maximum in the coefficient of thermal expansion. However, this situation is always a continuous crossover from one regime to another, as the glass transition is not a true thermodynamic phase transition. We plot the specific volume as a function of the temperature for ethane and propane (Figure 1) and for longer alkanes (Figure 2). We observe that there is a slope change in all these curves. Examination of the static radial distribution function shows that the state below the transition corresponds to a spatially disordered state. This observation precludes the possibility of the crystallisation transition and indicates that it corresponds to the glass transition. On the other hand, visual inspection of typical snapshots above and below the glass transition shows that chains do not experience any conformational change: the chains are entangled and appear in stretched configurations. By fitting the values of the specific volume as a function of the temperature by straight lines in limited ranges above and below the slope change we locate the glass transition of both fits. We observe that the glass transition temperature T_{g} increases with the chain length (see Figure 3), as it was obtained for more realistic models of linear alkanes [6]. On the other hand, as the chain is longer, the crossover range and the change on slope decreases. This fact makes more difficult to locate the glass transition by this procedure for long alkanes.

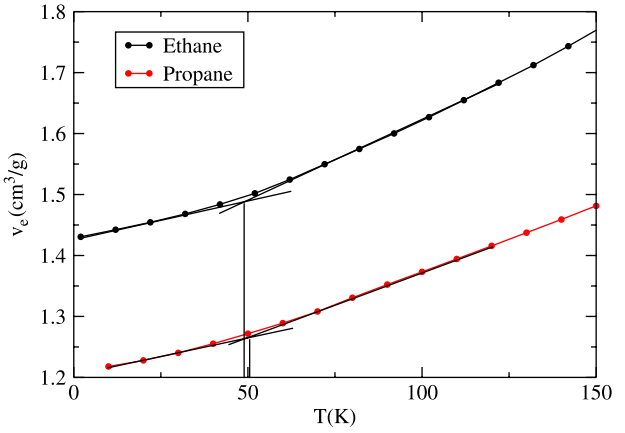

Figure 1. Plot of the specific volume as a function of the temperature for ethane (black filled circles) and propane (red filled circles). Lines are drawn through as a guide to the eye. The glass transition is estimated by the crossing of the best-fitted to the data straight thin lines below and above the glass transition.

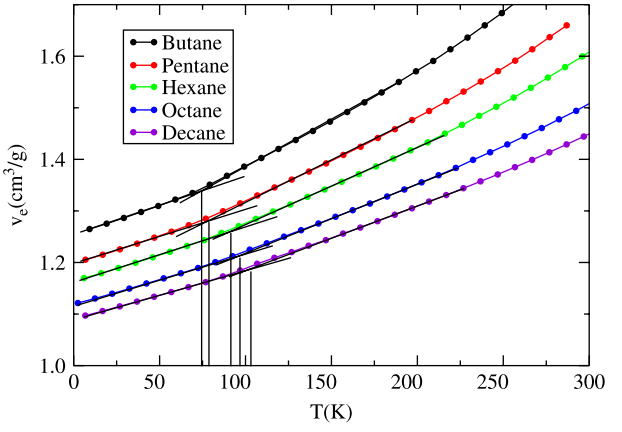

Figure 2. Plot of the specific volume as a function of the temperature for butane (black filled circles), pentane (red filled circles), hexane (green filled circles), octane (blue filled circles) and decane (violet filled circles). The glass transition is estimated by the crossing of the best-fitted to the data straight thin lines below and above the glass transition.

The glass transition has also an impact on the transport coefficients of the (supercooled) liquid. As the temperature approaches T_g, the self-diffusion coefficient vanishes and the shear viscosity diverges. Strictly speaking, we only observe a sudden decrease of D and increase of η. Figures 4 and 5 show the autocorrelation functions of the velocity and the pressure tensor for the pentane:

$$C_v(t) = \frac{1}{N}\sum_{j=1}^{N}\langle \mathbf{v}_i(0)\cdot\mathbf{v}_i(t)\rangle,$$
$$C_P(t) = \sum_{\alpha,\beta}\langle P_{\alpha\beta}(0)P_{\alpha\beta}(t)\rangle. \qquad (11)$$

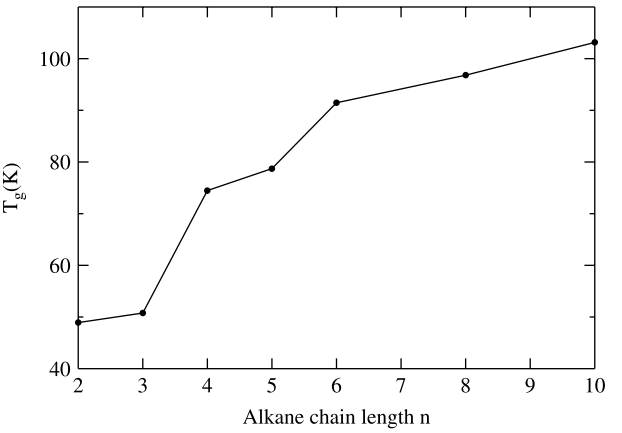

Figure 3. Glass transition temperature T_g as a function of the number of carbons of the alkane chain, obtained from the specific volume data in the cooling phase.

Similar curves are obtained for other alkanes. These correlation functions decay to zero as $t \to \infty$. As the temperature decreases, the velocity autocorrelation time changes from a monotonically decaying function to a structured function with two minima. On the other hand, the pressure autocorrelation function is always a monotonically decaying function, with a characteristic time scale which increases as the fluid is cooled. In order to get the self-diffusion coefficient D and the shear viscosity η, we calculate the cummulant of rescaled autocorrelation functions I_D and I_η:

$$I_D(t) = \frac{1}{3}\int_0^t \mathrm{d}\bar{t} C_v(\bar{t}), \quad I_\eta(t) = \frac{V}{10k_\mathrm{B}T}\int_0^t \mathrm{d}\bar{t} C_P(\bar{t}). \qquad (12)$$

Note that, formally $I_D \to D$ and $I_\eta \to \eta$ as $t \to \infty$. In practice, both cummulants reach a plateau for $t > \tau$, being τ the characteristic correlation time. This can be seen in the insets of Figures 4 and 5. However, for very large t the cummulant is affected by the statistical noise of the autocorrelation function (specially in the case of the pressure tensor), showing a somewhat erratic behaviour. As a consequence, we take as the transport coefficients the values of the cummulants when the plateau is reached. Visual inspection of the insets of Figures 4 and 5 confirms that D decreases and η increases as the temperature is reduced. For the smallest temperature $T = 76.92$ we could not obtain an estimation of the shear viscosity, as the pressure tensor autocorrelation does not decay to zero in the simulation time. Figure 6 shows the dependence of D and η with the temperature, and it confirms that D vanishes in the same temperature range than the sudden increase of η. Furthermore, this range is compatible with the glass transition temperature obtained from the specific volume data (see Figure 3). The Arrhenius plots of both properties seem to show an Arrhenius behaviour $\ln D \sim -\ln \eta \sim 1/T$

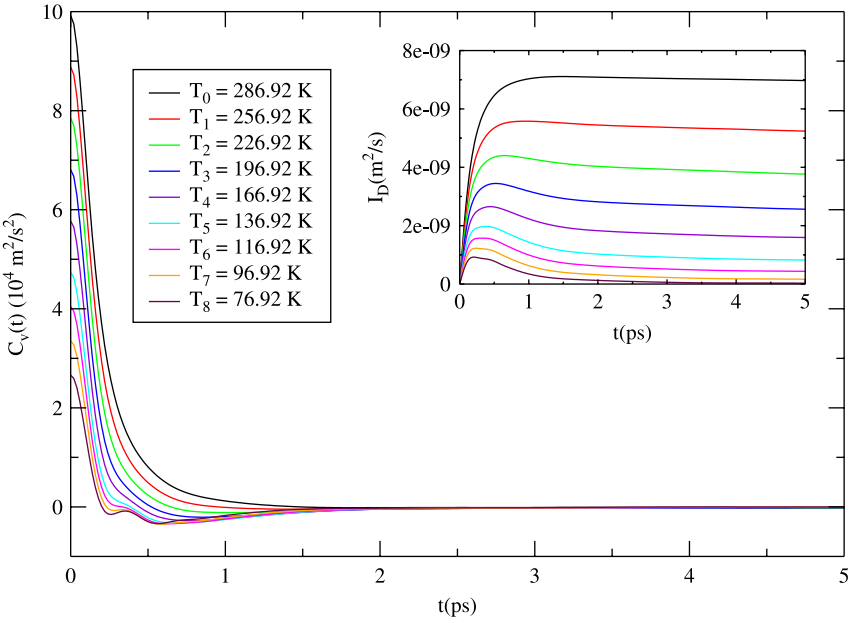

Figure 4. Velocity autocorrelation function for pentane for different temperatures. Inset: Rescaled cummulant of the velocity autocorrelation function (see text for explanation).

in the supercooled liquid regime before reaching the glass transition. However, the change in the slope close to the glass transition may indicate a Volger–Tamman–Fulcher behaviour $-\ln \eta \sim 1/(T - T_0)$ as predicted by the Adams–Gibbs theory. Further simulations in a range around the glass transition temperature would be required to characterise the behaviour of both transport coefficients close to the glass transition.

We finish our presentation of the simulation results by showing the behaviour of the orientational correlation functions g_1^e and g_2^e. As a typical case, we considered again the pentane case. Figures 7 and 8 show the results for $T = 286.92$ K where the equilibrium state of the system is a liquid, and $T = 96.92$ K, close to the glass transition, respectively. We note that, after an initial period, all the orientational correlation functions have an exponential decay, at least in the time range we considered. However, we cannot preclude the crossover to a more complex and slower decay in the correlations at longer times, as observed for realistic models of alkanes in the literature

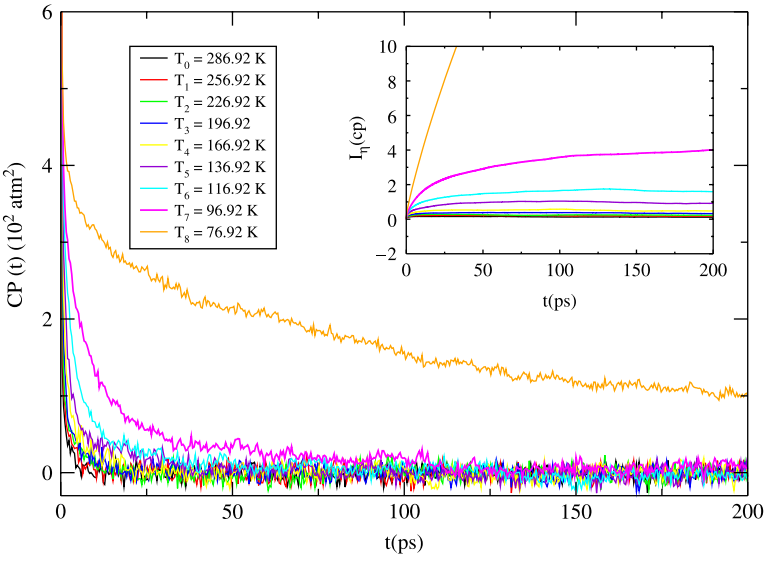

Figure 5. Pressure autocorrelation function for pentane for different temperatures. Inset: Rescaled cummulant of the pressure autocorrelation function (see text for explanation).

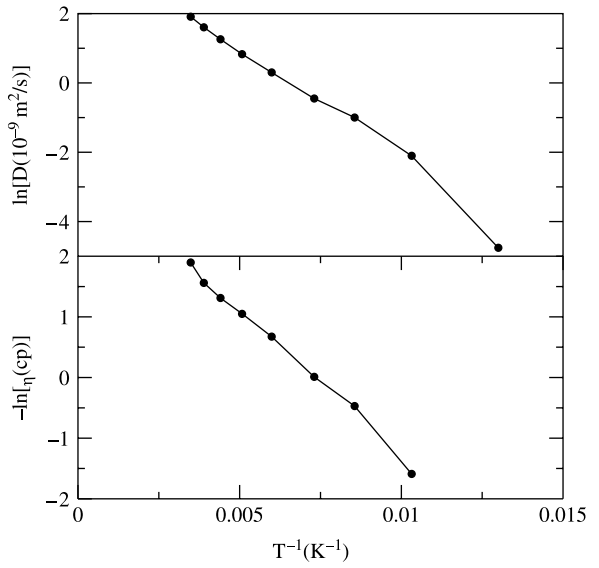

Figure 6. Upper panel: Arrhenius plot of the self-diffusion coefficient D for pentane. Lower panel: Arrhenius plot of the pentane shear viscosity η. Lines are drawn through as a guide to the eye.

[22,23]. Noticeably the behaviour of these functions at both temperatures is similar in the appropriate timescale, which is obviously much larger at the lower temperature than at the higher one. For the g_1 functions, we observe that the autocorrelation function for the bond and chord vectors decay slower than for the out-of-plane and the bisector vector, with autocorrelation times $\tau_1 = 4.78 \pm 0.02$ ps for $T = 286.92$ K, and 262.5 ± 0.7 ps for $T = 96.92$ K. With respect to the autocorrelation functions for the out-of-plane and the bisector vectors, they initially have a common behaviour (oscillatory for the high-temperature case, monotonically decaying with a correlation time of order of 30 ps for $T = 96.92$ K). However, for larger times $g_1^{\mathbf{s}}(t)$ (corresponding to the bisector vector) couples to the bond and chord autocorrelation functions. Although the autocorrelation time is of the same order in this later stage, the correlations are much smaller than for the bond and chord vector. Regarding the g_2 autocorrelation functions, at both temperatures and after a small initial period, we observe an exponential decay for all the vectors with the same autocorrelation time $\tau_2 = 1.82 \pm 0.03$ ps for $T = 286.92$ and 116 ± 1 ps for $T = 96.92$ K. The ratio between τ_1 and τ_2 is always larger than unity, and closer to the isotropic rotational diffusive limit $\tau_1/\tau_2 = 3$ for the higher temperature than for the lower temperature [6,23].

The behaviour of the orientational correlation functions is in agreement with the picture of the confinement of each alkane molecule into a pipe cage formed by their neighbours [6,23]. This explains that the autocorrelation functions associated with the bond and chord vectors decay slower than the other correlation functions. As the glass transition is approached, the timescale associated with the rearrangement of the alkane backbone experiences a sharp increase. This can be rationalised by the observation that backbone rearrangements are a cooperative phenomenon in dense phases, and they slow down near the glass transition.

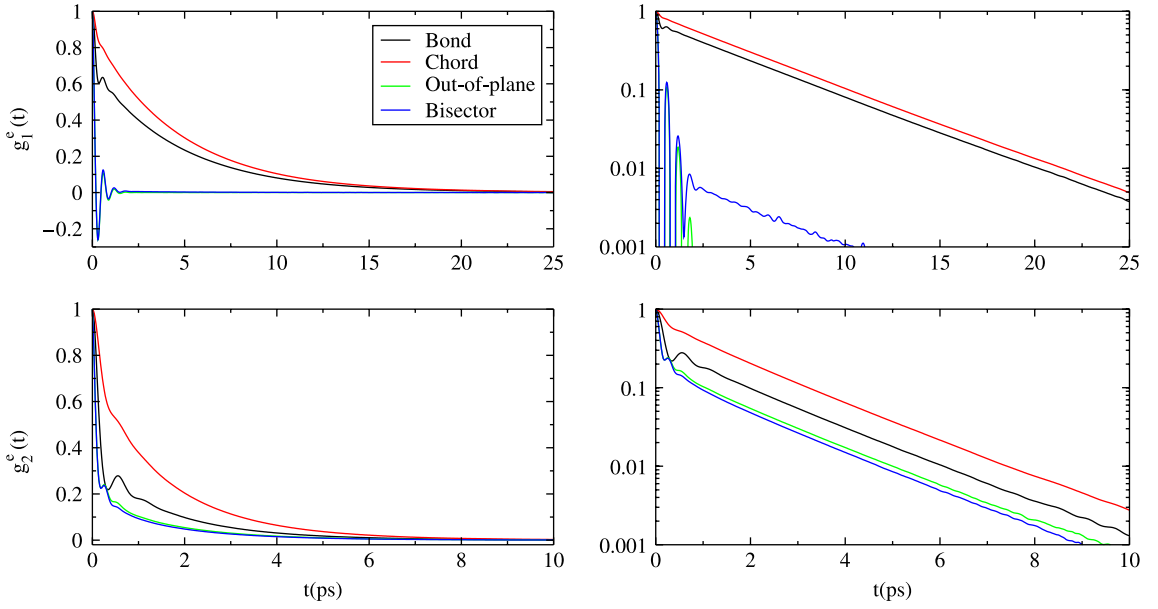

Figure 7. Orientational autocorrelation functions $g_1^{\mathbf{e}(t)}$ (upper row) and $g_2^{\mathbf{e}(t)}$ (lower row) for pentane at $T = 286.92$ K. The left panels correspond to a linear scale, and the right panels are the same plot in log-lin scale.

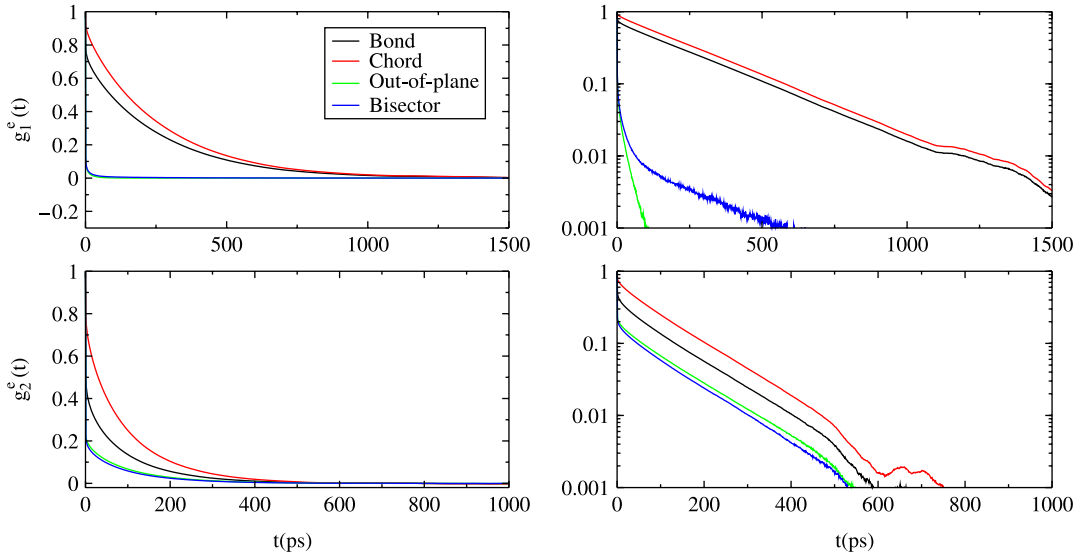

Figure 8. Orientational autocorrelation functions $g_1^{\mathbf{e}(t)}$ (upper row) and $g_2^{\mathbf{e}(t)}$ (lower row) for the pentane at $T = 96.92$ K. The left panels correspond to a linear scale, and the right panels are the same plot in log-lin scale.

4. Conclusions

In this paper, we present MD simulations of a flexible model of linear *n*-alkanes in which we turned off the bond bending and the torsional potential. We have localised the glass transition for $n = 2, \ldots, 10$ from the slope change in the specific volume, as well as from the behaviour of the self-diffusion constant D and the shear viscosity η. We observe an increase of the glass transition temperature as the alkane molecule is longer, in agreement with the predictions of more realistic models. On the other hand, we have studied the orientational autocorrelation functions associated with chain rearrangements. The functions associated with the backbone orientations (bond and chord vectors) decay slower than the corresponding functions to the bisector or out-of-plane vectors, with a characteristic autocorrelation time which increases as we approach the glass transition. This observation is in qualitative agreement with the predictions of more realistic models of alkanes, and it is explained by the picture of the alkane molecules confined into pipe cages formed by their neighbours. We can conclude that the bending or the torsional potentials are not essential to understand the physical mechanism for the glass transition of alkanes, although obviously they have an effect on it. Some previous studies [2,6] show that the glass transition temperature decreases as the torsional part of the intramolecular potential is turned off. As the torsional potential favours some conformations for each segment of the chain (trans, gauche), with energy barriers between them, the arrest of this degree of freedom occurs for higher temperatures than for the flexible model. We anticipate that this shift towards lower temperatures for the glass transition would be enhanced if we were to turn off the bending energy, as in the present case. However, we have not quantified this effect, and further work is needed to answer this question.

Acknowledgements

We acknowledge the financial support of Ministerio de Ciencia y Tecnología (Spain) through the Grant VEM2003-20574-C03-02, Ministerio de Educación y Ciencia (Spain) through the Grant ENE2007-68040-C03-02, and Junta de Andalucía through 'Plan Andaluz de Investigación' (Group FQM-205).

References

[1] P.G. Debenedetti, *Metastable Liquids: Concepts and Principles*, Princeton University Press, Princeton, 1996.
[2] D. Rigby and R.-J. Roe, *Molecular dynamics simulation of polymer liquid and glass. I. Glass transition*, J. Chem. Phys. 87 (1987), pp. 7285–7292.
[3] D. Rigby and R.-J. Roe, *Molecular dynamics simulation of polymer liquid and glass. II. Short range order and orientation correlation*, J. Chem. Phys. 89 (1988), pp. 5280–5290.
[4] D. Rigby and R.-J. Roe, *Molecular dynamics simulation of polymer liquid and glass. 3. Chain conformation*, Macromolecules 22 (1989), pp. 2259–2264.
[5] D. Rigby and R.-J. Roe, *Molecular dynamics simulation of polymer liquid and glass. 4. Free-volume distribution*, Macromolecules 23 (1990), pp. 5312–5319.
[6] R.J. Roe, *MD Simulation study of glass transition and short time dynamics in polymer liquids*, in *Advances in Polymer Science*, L. Monnerie and U.W. Suter, eds.,Vol. 116, Springer, Berlin/Heidelberg, 1996, pp. 111–144.
[7] M.G. Martin and J.I. Siepmann, *Transferable potentials for phase equilibria. 1. United-atom description of n-alkanes*, J. Phys. Chem. B 102 (1998), pp. 2569–2577.
[8] S.K. Nath, F.A. Escobedo, and J.J. de Pablo, *On the simulation of vapor-liquid equilibria for alkanes*, J. Chem. Phys. 108 (1998), pp. 9905–9911.

[9] B. Lobe, J. Baschnagel, and K. Binder, *Glass-transition in polymer melts – study of chain-length effects by Monte Carlo simulation*, Macromolecules 27 (1994), pp. 3658–3665.
[10] A. Galindo, C. Vega, E. Sanz, L.G. MacDowell, E. de Miguel, and F.J. Blas, *Computer simulation study of the global phase behavior of linear rigid Lennard-Jones chain molecules: comparison with flexible models*, J. Chem. Phys. 120 (2004), pp. 3957–3968.
[11] M.P. Allen and D.J. Tildesley, *Computer Simulation of Liquids*, Clarendon Press, Oxford, 1997.
[12] D. Frenkel and B. Smit, *Understanding Molecular Simulations: From Algorithms to Applications*, 2nd ed., Academic Press, San Diego, 2002.
[13] S. Melchionna, G. Ciccotti, and B.L. Holian, *Hoover NPT dynamics for systems varying in shape and size*, Mol. Phys. 78 (1993), pp. 533–544.
[14] W. Smith and T.R. Forester, *DL_POLY_2.0: a general-purpose parallel molecular dynamics simulation package*, J. Mol. Graph. 14 (1996), pp. 136–141.
[15] J.-P. Ryckaert, G. Ciccotti, and H.J.C. Berendsen, *Numerical integration of the cartesian equations of motion of a system with constraints: molecular dynamics of* n*-alkanes*, J. Comput. Phys. 23 (1977), pp. 327–341.
[16] J.R. Fox and H.C. Andersen, *Molecular dynamics simulations of a supercooled monatomic liquid and glass*, J. Phys. Chem. 88 (1984), pp. 4019–4027.
[17] M.S. Green, *Markoff random processes and the statistical mechanis of time-dependent phenomena. 2. Irreversible processes in fluids*, J. Chem. Phys. 22 (1954), pp. 398–413.
[18] R. Kubo, *Statistical-mechanical theory of irreversible processes. 1. General theory and simple applications to magnetic and conduction problems*, J. Phys. Soc. Jpn 12 (1957), pp. 570–586.
[19] D.J. Evans and G.P. Morriss, *Statistical Mechanics of Nonequilibrium Liquids*, 2nd ed., Australian National University E Press, Canberra, 1990.
[20] G. Marechal and J.P. Ryckaert, *Atomic versus molecular description of transport-properties in polyatomic fluids. Normal-butane as an illustration*, Chem. Phys. Lett. 101 (1983), pp. 548–554.
[21] P.J. Daivis and D.J. Evans, *Comparison of constant-pressure and constant volume nonequilibrium simulations of sheared model decane*, J. Chem. Phys. 100 (1994), pp. 541–547.
[22] K. Karatasos, D.B. Adolf, and S. Hotston, *Effects of density on the local dynamics and conformational statistics of polyethylene: a molecular dynamics study*, J. Chem. Phys. 112 (2000), pp. 8695–8706.
[23] H. Takeuchi and R.J. Roe, *Molecular dynamics simulation of local chain motion in bulk amorphous polymers. I. Dynamics above the glass transition*, J. Chem. Phys. 94 (1991), pp. 7446–7457.